Aerosol and Air Quality Research, 19: 2252–2266, 2019
Copyright © Taiwan Association for Aerosol Research
ISSN: 1680-8584 print / 2071-1409 online
doi: 10.4209/aaqr.2019.08.0410

Chemical Composition and Health Risk of $PM_{2.5}$ from Near-ground Firecracker Burning in Micro Region of Eastern Taiwan

Huazhen Shen[1,2], Chung-Shin Yuan[2*], Chun-Chung Lu[2], Yubo Jiang[2], Guohua Jing[1], Gongren Hu[1], Ruilian Yu[1]

[1] *College of Chemical Engineering, Huaqiao University, Xiamen, Fujian 361021, China*
[2] *Institute of Environmental Engineering, National Sun Yat-Sen University, Kaohsiung 804, Taiwan*

ABSTRACT

The randomness of firecracker-burning site and the overlapping impact of multi-sources makes the source apportionment of $PM_{2.5}$ during the firecracker burning events more difficult. To investigate the influences of the downwind distance to the firecracker-burning site on the temporospatial distribution of $PM_{2.5}$ and public health risk, $PM_{2.5}$ were sampled at three sites adjacent to a fixed firecracker-burning route accompanied with annual pilgrimage activity during the Lantern Festival in Taitung, Taiwan, which had a low background $PM_{2.5}$ concentration. The metallic elements, water-soluble ions, carbonaceous contents were analyzed. The potential sources were identified using positive matrix factorization. Finally, the health risks were assessed by calculating the hazard quotient and incremental lifetime carcinogenic risk, respectively. The results showed that the average concentration of $PM_{2.5}$ on the event days increased by approximately five-fold compared to the non-event days. The increase of chemical components varied significantly from the distance to the burning site. The concentrations of K, Fe, Al, Mg, K^+, Cl^- and OC rose by 6–14 times at one site close to a site with intensive firecracker burning, while increased by 2–6 times at one site far away from the firecracker burning sites. The $PM_{2.5}$ increment on the event days was mostly attributed to firecracker burning, kitchen fumes, and mobile sources. The health risk assessment results showed that the hazard index differed between the sampling sites. Furthermore, the cancer risk of one site close to the firecracker burning site was over the threshold, while that far away from the site was below the threshold.

Keywords: $PM_{2.5}$; Firecracker burning; Chemical composition; PMF; Health risk.

INTRODUCTION

Near-ground firecracker burning could cause a rapid and dramatic increase in $PM_{2.5}$ concentration, not only reducing ambient air quality and visual range but also posing hazards to residents' health. Moreover, other areas might suffer from $PM_{2.5}$ pollution by such firecracker burning because of long-range transport (Alexandre *et al.*, 2010; Tsai *et al.*, 2012). Previous literature reported that Asian megacities such as Beijing, Tianjin, Nanjing, New Delhi often suffer from highly polluted $PM_{2.5}$ episodes, accompanying more than several hundred μg m^{-3} during the traditional Chinese and Indian festivals (Zhang *et al.*, 2017b; Jung *et al.*, 2018; Mukherjee *et al.*, 2018; Rastogi *et al.*, 2019). During the festival, the concentration of various chemical indicators of firework displays increases dramatically. For instance, in Beijing, Ba, Cu, Pb as color agents, and propellants increased nearly 100 times (Liu *et al.*, 2019). Kong *et al.* (2015) found that organic carbon, elemental carbon, ammonium, potassium, and silicon accounted for nearly 70% of total $PM_{2.5}$ in the Spring Festival in Nanjing. Different from the spatiotemporal distribution, chemical compositions, and sources of $PM_{2.5}$ during traditional festivals in the megacities, a large number of near-gourd firecrackers are burned accompanying with blasting the God Handan or other folk performances as the pilgrimage activities occurred in the downtown area, a micro-region of Taitung City in Eastern Taiwan. The remarkable feature of $PM_{2.5}$ episodes in a micro-region is that the $PM_{2.5}$ influences in a short duration and distance. The distance from the sampling site to the firecracker burning site could cause large variation in the $PM_{2.5}$ spatial distribution, making the estimation of the firecracker burning contributed to $PM_{2.5}$ pollution more difficult. Additionally, regulated by local Environmental Protection Bureau, the pilgrimage routes are confined within the specified city blocks, and the firework burning sites are fixed as well. The areas near the pilgrimage are directly polluted by the firecracker burning, while the regions far away from the pilgrimage route are less affected by the firecracker burning. Therefore, it is of considerable significance to investigate the effects of the downwind

* Corresponding author.
Tel.: +886-7-5252000 ext. 4409; Fax: 886-7-52524409
E-mail address: ycsngi@mail.nsysu.edu.tw

distance to the burning site on the spatial distribution of $PM_{2.5}$ by choosing appropriate $PM_{2.5}$ sampling locations based on the pilgrimage routes.

The overlapping of multi-sources including local coal-fired power plants, metal processing factories, incinerators, as well as $PM_{2.5}$ from long-range transport in addition to firecracker burning during the festivals has made it even more challenging to clarify the contribution of firecracker burning to $PM_{2.5}$ pollution (Feng *et al.*, 2012; Yang *et al.*, 2014; Feng *et al.*, 2016). Kong *et al.* (2015) indicated that $PM_{2.5}$ pollution in Nanjing mainly comes from fireworks (50.0%), coal combustion (15.6%), soil (14.8%), vehicular exhaust (14.4%). Mukherjee *et al.* (2018) observed that in New Delhi firecracker burning in urban areas increased $PM_{2.5}$ concentration by more than 25% during the Diwali festival in 2016. Moreover, fine particles emitted from remote biomass burning through long-range transport also dramatically promote ambient $PM_{2.5}$. Compared to several industrial cities located in the western Taiwan, Taitung City has no heavy industries such as steelmaking, power generation, or waste incineration, and thus local $PM_{2.5}$ emission sources including coal-burning boilers, road dusts, traffic exhausts, kitchen fumes, and etc. dominate the $PM_{2.5}$ pollution. Furthermore, due to the barrier of the Central Range in Taiwan Island, Taitung City is rarely affected by $PM_{2.5}$ transported from outside the region (Fang *et al.*, 2010; Lee *et al.*, 2018). Therefore, Taitung City has low $PM_{2.5}$ concentration with an annual average $PM_{2.5}$ level of 9.7 μg m^{-3} for the past five years, which is even lower than the most stringent criteria of the annual average concentration of 10 μg m^{-3} (1T-3) allowed by United Nations (Fang *et al.*, 2013). Due to its low $PM_{2.5}$ background, Taitung City is selected for investigating the contribution of near-ground firecracker burning on $PM_{2.5}$ concentration.

A variety of metallic elements could be released in the firework displays (Tian *et al.*, 2014; Jiang *et al.*, 2015), which are used to generate colorful flame. Although the health risk assessment of heavy metals emitted from firework displays has been extensively investigated (Lin *et al.*, 2016; Song *et al.*, 2017; Zhang *et al.*, 2017a; Pong *et al.*, 2018; Zhang *et al.*, 2018b; Greven *et al.*, 2019), the risk assessment of heavy metals from near-ground firecracker burning has rarely been conducted. During the pilgrimage time in Taitung, "Blasting the God Handan", blessings and other exorcisms activities often attract an abundance of attendees at a pretty short distance. Therefore, firecracker burning may have a tremendous impact on the health of spectators but has mostly been overlooked (Wehner *et al.*, 2000; Ravindra *et al.*, 2003; Song *et al.*, 2006; Moreno *et al.*, 2007). Consequently, it is very imperative to assess the health risk of heavy metals emitted from firecracker burning on the spectators.

To investigate the impacts of the downwind distance to the burning site on the spatiotemporal distribution and the chemical composition of $PM_{2.5}$ during the Lantern Festival in Taitung City, we collected $PM_{2.5}$ samples in three periods (before, during, and after the firecracker burning) at three different sites, i.e., a site close to the burning site with intensive firecracker burning (site A), a site close to burning site but with non-intensive firecracker burning (site B), and a site far away from burning sites without firecracker burning (site C). The $PM_{2.5}$ concentrations and their metal components, water-soluble ionic (WSI), and carbonaceous species at the three sampling sites were analyzed. The potential sources and their contributions to $PM_{2.5}$ were analyzed by backward trajectory simulation and positive matrix factorization (PMF). The health risk of heavy metals in $PM_{2.5}$ emitted from firecracker burning was further assessed as well.

EXPERIMENTAL METHODS

Sampling Protocol

Three sites were selected for $PM_{2.5}$ manual sampling. As illustrated in Fig. 1, site A was a balcony on the second floor of a building neighboring an intensive firecracker burning site on the route of pilgrimage activities. Site B was a balcony on the third floor of a building close to a non-intensive firecracker burning site on the boundary of the path of pilgrimage activities, while site C was a balcony on the third floor of a building far away from sites A and B without firecracker burning at all. The distance between sites A and B was approximately 300 m, while that between sites A and C was about 450 m. The sampling periods set on February 21st and 24th, before and after the firecracker burning event, respectively, represented the non-event days (NDs) and the $PM_{2.5}$ samples were collected continuously for 24 h (from 8:00 to 8:00 of the next day). $PM_{2.5}$ samples collected on February 21st were denoted as A1, B1, and C1, and those received on February 24 were denoted as A4, B4, and C4. On February 22nd and 23th, which were the event days (EDs) during the Lantern Festival when pilgrimage activities were held, the samples were collected from 14:00 to 24:00. From the midnight (0:00) to the next morning (8:00), no firecracker burning was conducted. To avoid low $PM_{2.5}$ concentration from the midnight to the early morning dragging down the average $PM_{2.5}$ level of the event day, $PM_{2.5}$ samples were not collected at that time. $PM_{2.5}$ samples collected on February 22nd were denoted as A2, B2, and C2, while those samples collected on February 23rd were denoted as A3, B3, and C3. $PM_{2.5}$ was sampled using the $PM_{2.5}$ sampler (BGI, PQ200) with WINS impactors under an air flow rate of 16.7 L min^{-1}. Each quartz fiber filter of 47 mm diameter was conditioned in the desiccators at constant room temperature (25 ± 3°C) and relative humidity (45 ± 5%) for at least 24 h and further weighted by an analytical microbalance (Sartorius MC 5) with a mass precision of 10^{-6} gram before and after $PM_{2.5}$ sampling.

In addition to the three aforementioned sampling sites, we also conducted on-line monitoring of $PM_{2.5}$ and PM_{10} concentrations by a real-time particulate monitor (Met-one, Aerocet 531S) along the pilgrimage route during the firecracker burning activities on the EDs.

Chemical Composition Analysis

Prior to analyzing the metallic elements in $PM_{2.5}$, a sheet of 1/2-sized quartz filter paper was placed in a 120 mL vessel for conducting microwave digestion with 30 mL of an acid mixture [HNO_3 (v/v% = 65%): $HClO_4$ (v/v % = 70%) = 3:7, v/v] at 150–200°C for 2 h. After that, 25.0 mL of ultrapure water was added to rinse off the residual acids,

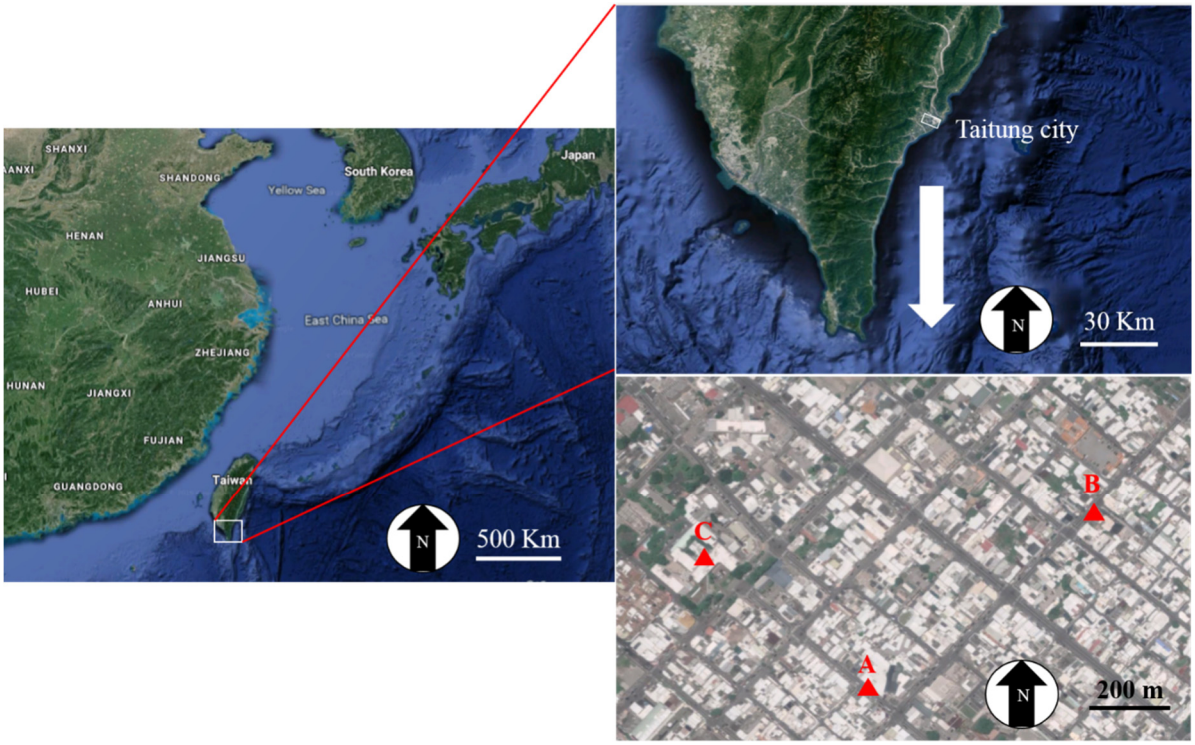

Fig. 1. Location of three sampling sites selected for collecting $PM_{2.5}$ at Taitung, Taiwan.

then the digestion and rinse processes were repeated for three times, and finally, the solution was diluted to 30 mL with 0.5 mol L^{-1} HNO_3 for further metallic analysis. Sixteen metallic elements (Mg, Al, Ca, Ti, Mn, Fe, Ni, Zn, Pb, Cr, Cd, K, As, Ni, Cu, and Na) were analyzed using an inductively coupled plasma-atomic emission spectrometer (ICP-AES) (PLASMA 400, PERKIN ELMER) (Wu *et al.*, 2015).

Before analyzing the WSIs, a quarter of the quartz filter was placed in a 50 mL polyethylene (PE) bottle, 30 mL deionized water (DI H_2O) was added, and the mixture was sonicated for 120 min. The solution was further filtered with a 0.45 μm acetate fiber filter, and the filtrate was analyzed for ionic species using an ion chromatography (Dionex, Series 120). The measurement method with operating parameters were described in detail by previous research (Li *et al.*, 2013a).

The carbonaceous species in $PM_{2.5}$ were analyzed using an elemental analyzer (CHNS/O 1108, Carlo Erba) with an autosampler (Model AS 200) and a DP 700 integrator. The elemental carbon (EC) and total carbon (TC) in $PM_{2.5}$ were determined, and organic carbon (OC) was estimated by subtracting EC from TC. The preparation method was described detailly in previous research (Yang *et al.*, 2017).

Quality Assurance (QA) and Quality Control (QC)

The filters and other consumables were supplied with backups. All instruments and filters were carefully installed prior to sampling. All items involved sampling operation such as the starting and ending time of PQ200, sampling flow rate, weather conditions, and etc. were recorded so that the operating parameters were available for checking to accurately determine the $PM_{2.5}$ concentration. To ensure the accuracy of chemical analysis experiments, the spiking method was performed in which a specific amount of standard reagent was spiked into the samples for the detection of chemical compositions under the same analytical conditions. Each measurement was repeatedly analyzed to obtain the recovery rate. The closer the recovery rate approached to unity, the higher the accuracy of the analytical instrument is (Tsai *et al.*, 2010; Lin *et al.*, 2013; Yuan *et al.*, 2006).

Relative Abundance Analysis

Relative abundance analysis (R_a) is the ratio of the percentage of the target metallic elements in $PM_{2.5}$ of the EDs over that in the NDs, as shown in Eq. (1) to identify the enriched metal influenced by the firecracker burning but not by other pollution sources (Kong *et al.*, 2015; Liu *et al.*, 2019).

$$Ra = \frac{C_{FC}^{i} / C_{FC}^{\mathrm{PM2.5}}}{C_{n-Fc}^{i} / C_{n-FC}^{\mathrm{PM2.5}}} \quad (1)$$

where C^{i}_{FC} and $C^{PM2.5}{}_{FC}$ (μg m^{-3}) are the average concentrations of a target metallic element i and $PM_{2.5}$, respectively, in the EDs; $C^{i}_{n\text{-}FC}$ and $C^{PM2.5}{}_{n\text{-}FC}$ (μg m^{-3}) are the average concentrations of the corresponding metallic element i and $PM_{2.5}$ in the NDs, respectively.

Backward Trajectory Simulation

In order to trace the air masses transported toward Taitung City, backward trajectories from the reception sites are commonly used to identify their potential source regions. The Hybrid Single-Particle Lagrangian Integrated Trajectory (HYSPLIT) was employed to trace the transport routs of the

air parcel arriving at Taitung City on February 21st–24th in this study. Three-dimensional (height, longitude, and latitude) and 72-h backward trajectories were simulated every 6 h from 18:00 UTC, February 20th (Li *et al.*, 2017a). Air masses with low altitude of 100, 300, and 500 m were simulated. Finally, a total of 24 simulated back trajectories were plotted for this study.

Positive Matrix Factorization

PMF5.0 was employed to quantify the mass contribution of the chemical constitutes during the EDs and NDs as shown in Eq. (2).

$$X = G \times F + E \tag{2}$$

To evaluate the fitting degree of PMF, Q is the goodness-of-fit parameter which can be obtained by Eq. (3),

$$Q = \left(\frac{E}{U_{nc}} \right)^2 \tag{3}$$

where U_{nc} is the uncertainty matrix of each chemical species and can be calculated by Eq. (4) (U.S. EPA, 2014),

$$U_{nc} = \sqrt{\left(EF \times conc.\right)^2 + \left(0.5 \times MDL\right)^2} \tag{4}$$

where EF is the determined error fraction, which was set as 10% in this study (Yang *et al.*, 2015; Li *et al.*, 2017b). A total of twelve samples were divided into two groups representing the $PM_{2.5}$ concentrations of EDs and NDs, respectively. Twenty-six chemical species were introduced into the PMF model for analyzing their contribution. A total of 20 times was run with the number of factors ranging from 3 to 6 and determined by the Q value, residual analysis, and correlation analysis between the observed and predicted values. To increase the Q value, the rotations were performed by selecting an appropriate number of the factors with the strength ranged from –1.0 to 1.0. The simulated results of source apportion with the highest values of Q (Robust) and Q (True) was chosen as the $PM_{2.5}$ source profiles during the NDs or EDs.

Health Risk Assessment of Heavy Metals in $PM_{2.5}$

To evaluate the non-carcinogenic health risk, the inhalation (D_{inh}) for adults and children was determined based on an individual's body weight and exposure span as shown in Eq. (5) (Wang *et al.*, 2007; Zhang *et al.*, 2018a):

$$D_{inh} = \frac{C \times InhR \times EF \times ED}{BW \times AT} \tag{5}$$

where C (mg m^{-3}) is the average concentration of metallic species in $PM_{2.5}$ sampled on February 22nd and 23rd; D_{inh} (mg $kg^{-1} \cdot day^{-1}$) is the exposure dosage by respiratory inhalation; InhR is the inhalation rate of 7.6 and 20 m^3 day^{-1} for children and adults, respectively; EF is the exposure frequency and once every year (day $year^{-1}$) was adopted for representing the EDs in this study; ED is the exposure duration of 6 and 24 years for children and adults, respectively; BW is the average body weight of 15 and 70 kg for a child and adult, respectively; AT (day) is the average time for non-carcinogenic toxic risks as shown in Eq. (6),

$$AT = ED \times 365 \tag{6}$$

Hazard Quotient (HQ) representing non-carcinogenic risk is determined using Eqs. (7) and (8):

$$HQ = \frac{D_{inh}}{R_{fD}} \tag{7}$$

$$HI = \sum HQ_i \tag{8}$$

where R_{fD} (mg kg^{-1} day^{-1}) is the reference dose. The R_{fD} values are 3.01×10^{-4}, 1.0×10^{-3}, 2.86×10^{-5}, 1.4×10^{-5}, 2.06×10^{-2}, 3.52×10^{-3}, 7.0×10^{-3}, and 3.01×10^{-1} for As, Cd, Cr, Mn, Pb, Ni, V, and Zn, respectively (Feng *et al.*, 2016). The Hazard index (HI) can be obtained by summing up the HQ of single metal to estimate the total risk. If HI ≤ 1, there is no adverse effect of $PM_{2.5}$ on human health, while there is if HI > 1.

For carcinogenic risk, it is determined by the following Eqs. (9) and (10):

$$R_i = LADD \times SF_a \tag{9}$$

$$R_t = \sum R_i \tag{10}$$

where R_i is the carcinogenic risk caused by specific metal element i; LADD (mg kg^{-1} day^{-1}) is the lifetime average daily dosage of single heavy metals exposure by inhalation which is described as Eq. (11),

$$LADD = \frac{C \times EF}{AT} \times \left(\frac{InhR_{child} \times ED_{child}}{BW_{child}} + \frac{InhR_{adult} \times ED_{adult}}{BW_{adult}} \right) \tag{11}$$

where SF_a (kg·day mg^{-1}) is the slope factor with the values of 15.1, 6.4, 42, and 0.84 for As, Cd, Cr, and Ni, respectively (Wang, 2007); R_t is the total of carcinogenic risk exposure to humans.

RESULTS AND DISCUSSION

$PM_{2.5}$ Concentration Analysis

The daily average $PM_{2.5}$ concentration of A1 (15.9 μg m^{-3}) was higher than those of B1 (11.8 μg m^{-3}) and C1 (10.3 μg m^{-3}) on February 21st during the NDs as shown in Fig. 2(a), because site A is located at the downtown of Taitung City with many restaurants and traffics, while the flow of people and traffic is relatively fewer around sites B and C. Additionally, site A is situated at the downwind of site C on February 21st as the wind mainly blew northwesterly or northwest-westerly (see Fig. S1(a)). Thus, the average $PM_{2.5}$ concentration of

C1 was less influenced by the transport of $PM_{2.5}$ from the downwind site A.

The daily average $PM_{2.5}$ concentrations of A2 (70.0 μg m^{-3}) and B2 (30.0 μg m^{-3}) on February 22nd, A3 (59.1 μg m^{-3}) and B3 (47.6 μg m^{-3}) on February 23rd were significantly higher than those on February 21st, when a vast number of firecrackers were burned along the pilgrimage activities on the EDs. Additionally, the daily average $PM_{2.5}$ concentrations of A2 was much higher than that of B2, probably because site A was more adjacent to the intensive firecracker burning sites, while a relatively smaller amount of firecracker was burned around site B. The daily average $PM_{2.5}$ concentrations of C2 (23.4 μg m^{-3}) and C3 (17.7 μg m^{-3}) were the lowest among three sampling sites, because on the one hand, the pilgrimage activities and the firecracker burning were banned at site C on February 22nd and 23rd; on the other hand, site C was still located upwind of site A when Taitung was dominated by northwest and west wind with low speed during the EDs (see Figs. S1(b)–S1(c)). On February 24th, after ending the pilgrimage activities, the average $PM_{2.5}$ (24.0 μg m^{-3}) of A4 was not influenced by firecracker burning anymore but was still higher than those of B4 (19.5 μg m^{-3}) and C4 (13.8 μg m^{-3}), which was as similar as the distribution character on February 21st.

The results of continuous monitoring of $PM_{2.5}$ and PM_{10} show that the near-ground mean concentrations of $PM_{2.5}$ and PM_{10} reached up to 32 ± 10 μg m^{-3} and 102 ± 20 μg m^{-3}, respectively, before one completed process of firecracker burning around site A. The higher concentrations of $PM_{2.5}$ could be attributed to the heavier cooking fumes and traffic exhaust accompanying with the pilgrimage activities than the NDs on February 22nd (see Fig. 2(b)). When a large number of firecrackers was set off, the atmospheric concentrations of $PM_{2.5}$ and PM_{10} rapidly increased to 613 μg m^{-3} and 2,049 μg m^{-3} in two minutes, and then slowly decreased to 22 μg m^{-3} and 93 μg m^{-3}, respectively. The phenomenon inferred that the mean concentration of $PM_{2.5}$ before and after the cracker burning contributed by the heavy traffic flow, and cooking fumes was much lower than the daily average $PM_{2.5}$ of 70 μg m^{-3} at site A. Therefore, the daily average concentrations of $PM_{2.5}$ at site A during the EDs were substantially attributed to the elevation caused by the continual high-concentration peak of $PM_{2.5}$ during the firecracker burning.

Metallic Element Analysis

The mean metallic content in $PM_{2.5}$ sampled at sites A, B, and C during the NDs accounted for 13.4 ± 2.4% of total $PM_{2.5}$ concentration, while that at sites A, B, and C significantly

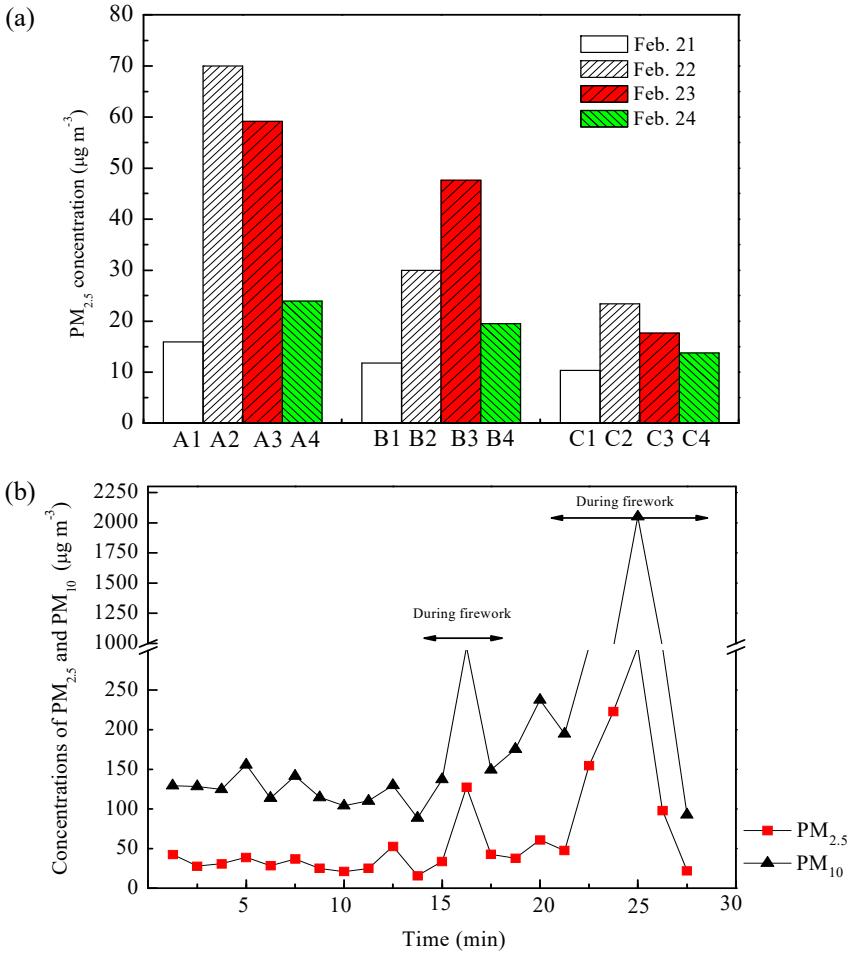

Fig. 2. Variation of $PM_{2.5}$ concentrations (a) daily average concentration at three sampling sites during sampling period; (b) real-time concentrations of $PM_{2.5}$ and PM_{10} concentrations during a firecracker-burning process.

increased to 22.8 ± 2.8% during the EDs due to firecracker burning. The mean concentration of each metallic element in $PM_{2.5}$ of A2 and A3, denoted as $(C_{iA2} + C_{iA3})/2$, at site A during the EDs was much higher than that of A1 and A4, denoted as $(C_{iA1} + C_{iA4})/2$ (see Fig. 3(a)). The mean concentrations of K, Mg, Fe, and Al during the EDs were approximately 6-times higher than those during the NDs. Potassium is mainly originated from the oxidizing agents of firecrackers such as KNO_3, $KClO_3$, and $KClO_4$, the oxidation of carbon and sulfur in powder which is a basic chemical reaction occurred when firecracker is exploded (Chen *et al.*, 2016; Yang *et al.*, 2018). Powdered Mg and Al are the common reducing reagents of firecrackers (Vecchi *et al.*, 2008; Wang *et al.*, 2013). Iron is often used as the propellant of firecrackers in the form of ferrocene (Han *et al.*, 2019). The average concentrations of Ti, Mn, Cr, Ca, Na, V, Zn, Cd, and Cu at site A during the EDs were 3-times higher than those during the NDs. The rise of Ca, Na, Cu, Ti, Zn, and Cr concentrations could be attributed to the occasional burning of a few small fireworks displayed along with the pilgrimage since they are the main coloring agents of firework (Lin *et al.*, 2016); the increase of Cd was majorly attributed to traffic exhausts (Pong *et al.*, 2018). It's noted that a few metallic elements as mentioned could be emitted by other sources. For instance, Iron and Titanium are the major crustal elements and thus could be released from the fugitive road dust during the EDs (Li *et al.*, 2012, 2015); Sodium might be released from the sea salts during the cooking activities in dry and high-temperature condition such as meat roasting (Zhang *et al.*, 2016); Zinc might also be released from the tire wear of vehicles (Lough *et al.*, 2005; Hjortenkrans *et al.*, 2007).

The increments of metallic elements at sites B and C were lower than those at site A as shown in Figs. 3(b)–3(c). The concentrations of Al, Na, and Mg at site B raised by approximately 3-times while the concentrations of Cu, Zn, K, Ca, Cd, Cr, Ti, Fe, and Mn increased by about 2-times during the EDs. At site C, although the concentrations of Al and Mg increased by about 4-times during the EDs, most of the metallic elements such as Fe, Na, Cd, Cr, Cu, Mn, Ca, Zn, and K increased approximately by 2-times. Therefore, the temporal distribution of metallic elements was substantially influenced by the distance of the sampling site to the burning site. The shorter distance was between the sampling site and the burning site, the larger the increment of metallic elements was formed in the $PM_{2.5}$. However, the concentration increment of Ni during the EDs was the smallest at each sampling site, and merely 1.5-times higher than those during the NDs; what's more, their concentrations even decreased on February 23rd compared to that during the NDs, indicating that the concentration of Ni was less influenced by firecracker burning. It's known that Ni mainly originated from coal or heavy oil-burning boilers (Kong *et al.*, 2015; Yang *et al.*, 2017), and thus the contribution from coal or heavy oil-burning boilers was much lower than the other pollution sources to the form of $PM_{2.5}$ during the EDs.

To further investigate the characteristics and abundance of metallic elements in $PM_{2.5}$ around the sampling sites, the relative abundance (R_a) of metallic elements were determined. It showed that the most significantly abundant metallic elements in $PM_{2.5}$ with $R_a > 2$ at site A were K, Cd, Mg, Fe, and Al, confirming that they were mainly released from the firecracker burning (see Fig. 3(d)), while the R_a of other metallic elements such as Mn, Cr, Na, V, Zn, Ti, and Cu were higher than unity, indicating that the metallic elements released from firework display, traffic exhaust, kitchen fumes and etc. were enriched in $PM_{2.5}$, but lower than those emitted from firecracker burning. Additionally, the Ra of Ni was lower than unity at site A, confirming that the influence of coal- or heavy oil-fired boilers on $PM_{2.5}$ was much lower than other emission sources such as firecracker burning, firework display, traffic exhaust, cooking fume.

At site B, the R_as of Na, K, Al, and Mg were nearly equal to or slightly lower than unity, indicating that the concentrations of these metallic elements at site B were less affected by firecracker burning than those at site A. However, the R_as of Al and Mg at site C were much higher ($R_a > 2$), while those of Na, K, Zn, Fe, Ni, Ca, and Cd were slightly higher than unity. The results indicate that many metallic elements were also much abundant in $PM_{2.5}$ at site C, inferring that the large proportion of $PM_{2.5}$ at site C was influenced by the dispersion of $PM_{2.5}$ from the intensive burning sites.

Water-soluble Ion (WSI) Analysis

The variation of WSI in $PM_{2.5}$ sampled at sites A, B, and C is shown in Fig. 4. During the NDs, the mean concentrations of WSIs at sites A, B, and C were 6.2 ± 1.5, 5.8 ± 2.0, and 3.5 ± 0.6 μg m^{-3} which accounted for 31.2 ± 1.4%, 37.4 ± 0.3% and 28.9 ± 0.6% of the total mass of $PM_{2.5}$, respectively. During the EDs, the mean concentrations of WSI at sites A and B significantly increased by 5.0- and 2.7-times and reached up to 31.2 ± 4.2 and 15.9 ± 5.3 μg m^{-3}, respectively. The contents of WSI in $PM_{2.5}$ sampled at sites A and B accounted for 48.2 ± 4.3% and 41.0 ± 2.1%, respectively, indicating that both the concentrations and contents of WSIs were promoted by the intensive firecrackers burning. While, the mean concentration of WSIs (7.5 ± 2.9 μg m^{-3}) at site C during the EDs was approximately 2.2-times higher than that (3.5 ± 0.6 μg m^{-3}) during the NDs, indicating that site C was far away from the firecracker burning site, however, the concentrations of WSIs in $PM_{2.5}$ still increased, merely the increment was lower than those at sites A and B.

The concentration variation of WSIs at site A is shown in Fig. 4. It shows that the mean concentrations of K^+ and Cl^- at site A during the EDs were 11.6- and 7.5-times higher than those during the NDs, respectively, resulting from the oxidation of charcoal in contact with KNO_3, $KClO_4$, and $KClO_3$ during the firecracker burning as shown in Eq. (12):

$$KClO_4 + 2C \rightarrow KCl + 2CO_2 \quad (12)$$

The concentrations of SO_4^{2-} at site A during the EDs were about 4.5-times higher than those during the NDs due to the oxidation of elemental sulfur powder by KNO_3 as shown in Eq. (13):

$$10KNO_3 + 8C + 3S \rightarrow 2K_2CO_3 + 3K_2SO_4 + 6CO_2 + 5N_2 \quad (13)$$

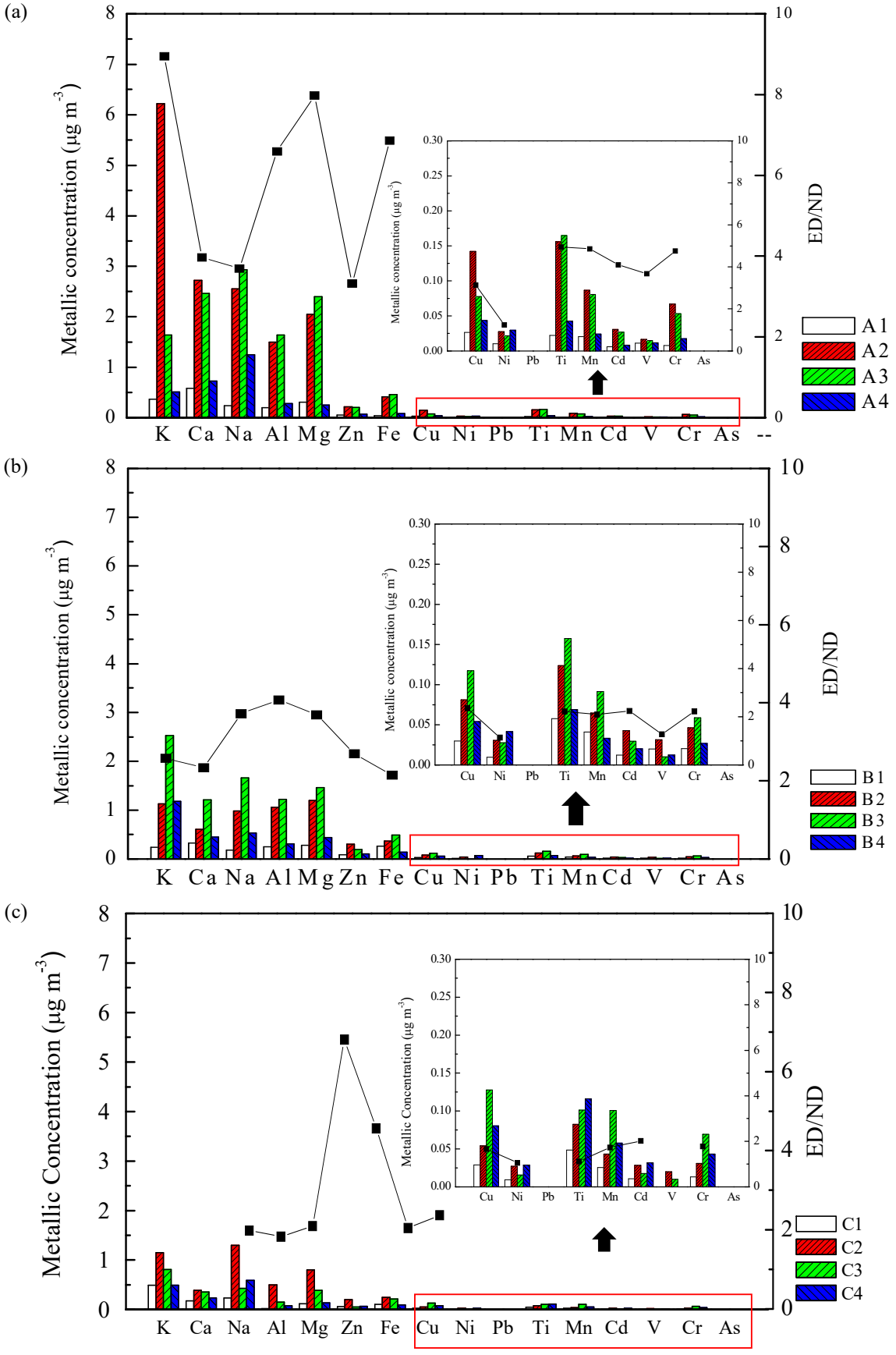

Fig. 3. Variation of daily metallic element concentrations at (a) site A; (b) site B; (c) site C; and (d) R_a for three sampling sites.

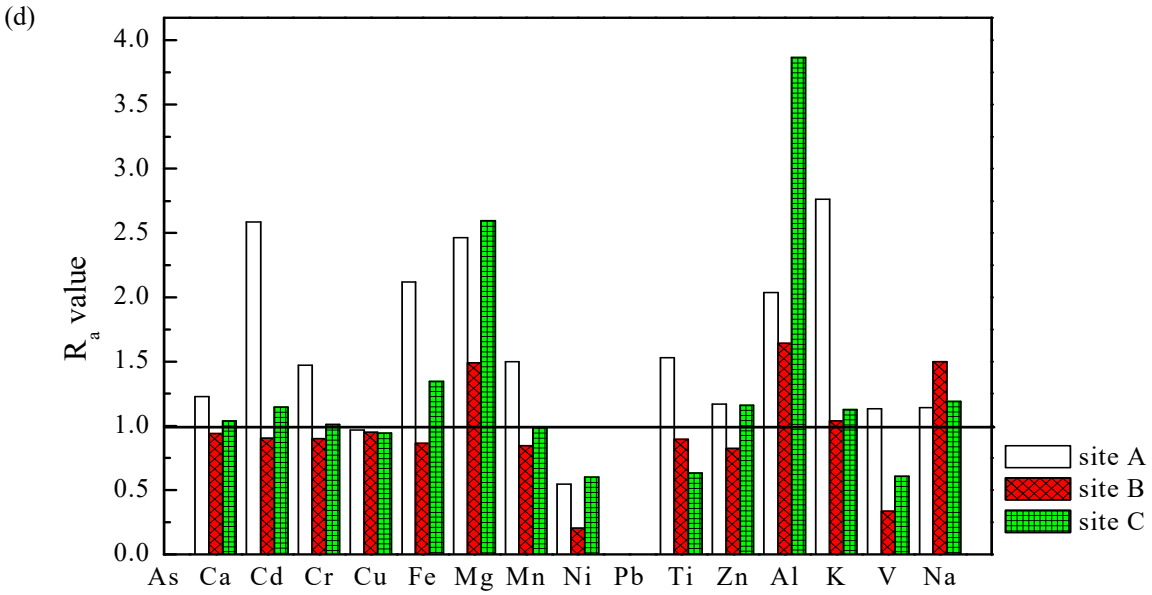

Fig. 3. (*continued*).

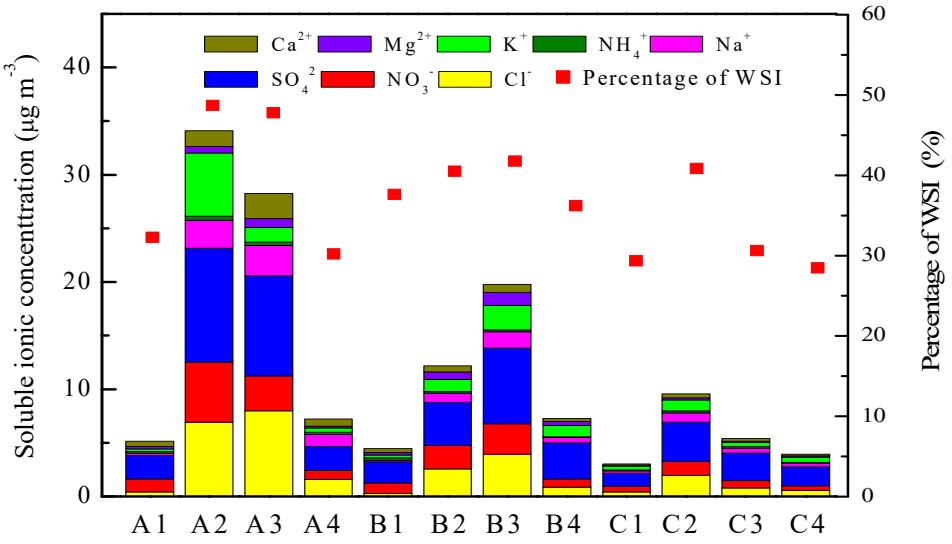

Fig. 4. Variation of daily WSI concentrations at three sampling sites.

The mean concentrations of NO_3^-, Na^+, Mg^{2+}, and Ca^{2+} at site A during the EDs were 4.4-, 3.8-, 3.7-, and 3.1-times higher than those during the NDs, respectively. It was noted that the mean concentration of NH_4^+ during the EDs was also 2-times higher than that during the NDs, which was probably ascribed to the oxidation of elemental sulfur powder by NH_4ClO_4 as shown in Eq. (14):

$$NH_4ClO_4 + 2S \rightarrow NH_4\,Cl + 2SO_2 \quad (14)$$

In addition, NH_4^+ might be emitted from snack-street boiling because a small amount of ammonium chloride or ammonium phosphate as food ingredients are also used to increase the toughness of noodles (Li *et al.*, 2014).

At site B, the mean concentrations of Cl^-, Na^+, and K^+ during the EDs were 5.6-, 3.7-, and 2.5-times higher than those during the NDs, respectively, and 2.9-times, 2.8-times, 2.2-times, and 2.1-times higher than those of Mg^{2+}, NO_3^-, Ca^{2+}, and SO_4^{2-} during the NDs, respectively (see Fig. 4). The results indicate that the increments of WSIs were much lower than those at site A. At site C, the increments of WSIs were far lower than those at sites A and B (see Fig. 4), revealing that the increments of WSIs differed significantly among sites A, B, and C, which were the same as metallic elements due to the variation of the distance between sampling site and burning site.

As shown in Table S1 the mass ratios of K/K^+ of A1 and A4 were 1.6 and 1.2 during the NDs, respectively while those of A2 and A3 were 1.0 and 1.1 during the EDs, indicating that the large proportion of K existed in the form of ions, such as KCl, K_2SO_4, and KNO_3, rather than those in the form of metallic element in $PM_{2.5}$ after the massive

explosion of firecrackers, which was in an agreement with Zhang *et al.*' (2018b) observation. The mass ratios of Mg/Mg^{2+} of A1 and A4 were 1.3 and 1.5, while those of A2 and A3 reached up to 3.4 and 2.9, respectively, indicating that most of Mg was not converted to Mg^{2+} after the firecracker explosion. The metallic element of Mg was probably originated from the residual Mg powder due to the incomplete explosive reaction of Mg alloy. In addition, the mass ratios of Cl^-/Na^+ of A1 and A4 during the NDs nearly equal to unity, approaching to the equivalent ratio of sea salts, but increased to 1.5 and 1.6 of A2 and A3 during the EDs, respectively, resulting from the rapid release of Cl^- which then probably existed in the form of KCl after firecracker burning. Therefore, during the EDs, the metallic element of Mg, the ion of K^+, and the ratio of Cl^-/Na^+ are suitable to indicate firecracker burning.

Carbonaceous Content Analysis

During the NDs, the mean total carbon (TC) contents in $PM_{2.5}$ at sites A, B, and C accounted for 11.9 ± 2.3%, 10.1 ± 1.4%, and 11.7 ± 0.5%, respectively. During the EDs, the mean TC content at site A increased to 22.5 ± 2.3% (see Fig. 5), indicating that the TC content in $PM_{2.5}$ at site A was significantly elevated by the firecracker burning. Although the mean TC contents increased to 15.7 ± 0.7% and 16.2 ± 1.7% at sites B and C, they were less elevated than that at site A.

During the EDs, the mean contents of OC and EC at site A were 11.6 ± 0.8 and 2.8 ± 0.5 μg m^{-3}, respectively, and 6.7- and 3.9-times higher than OC (1.7 ± 0.8 μg m^{-3}) and EC (0.7 ± 0.2 μg m^{-3}) during the NDs. The mean contents of OC (4.7 ± 1.7 μg m^{-3}) and EC (1.4 ± 0.5 μg m^{-3}) at site B during the EDs were 4.15- and 2.98-times higher than OC (1.1 ± 0.5 μg m^{-3}) and EC (0.5 ± 0.2 μg m^{-3}) during the NDs, respectively. The mean contents of OC (2.5 ± 0.8 μg m^{-3}) and EC (0.9 ± 0.2 μg m^{-3}) at site C were 3.4- and 2.4-time higher than OC (0.7 ± 0.1 μg m^{-3}) and EC (0.4 ± 0.2 μg m^{-3}) at site C. The results confirmed that the distance between the sampling site and the burning site played an essential role in the spatial distribution of the contents of $PM_{2.5}$ released from firecracker burning, namely, the longer the distance was, the lower the concentration increments of OC and EC in $PM_{2.5}$ were.

The mean mass ratio of OC/EC during the EDs was 4.2 ± 1.0 and significantly higher than that (2.4 ± 0.4) during the NDs at site A. The OC/EC ratios during the EDs approached 3.1–5.7 for firecracker burning observed by Feng *et al.* (2016), but much lower than 7.3 for wood burning (Choosong *et al.*, 2010), suggesting that the firecracker burning as the primary $PM_{2.5}$ source had played an essential role in the form of organic carbon during the Lantern Festival. The OC/EC ratio of 3.2 ± 0.2 during the EDs was also higher than that (2.3 ± 0.1) during the NDs at site B. It shows that the concentrations of OC and EC increased significantly, particularly for OC which increased much higher than that of EC. It was probably that the burning of organic matter in firecracker such as phenolic resin, polyvinyl alcohol, polyoxyethylene would release a large amount of OC to the atmosphere through the explosion. The OC/EC ratio (2.7 ± 0.3) at site C during the EDs was much lower than those at sites A and B, which could be attributed to that site C was far away from the burning site.

It is noteworthy that the OC/EC ratio at site A was much higher than that at site B, indicating that the carbonaceous species in $PM_{2.5}$ at site A was not only influenced by $PM_{2.5}$ released from firecrackers burning, but also by $PM_{2.5}$ with higher ratio of OC/EC emitted from other anthropogenic activities. It is known that the OC/EC ratio of $PM_{2.5}$ released from various cooking activities such as meat roasting, cafeteria frying, and snack-street boiling, ranged from 8.8 to 55 since a large number of OC are released through oxidation, decarboxylation, and cyclization reactions from the raw oil and meat components (Li *et al.*, 2014). Compared to site B, the OC/EC ratios of $PM_{2.5}$ at site A increased dramatically due to potential proliferated cooking activities during the EDs.

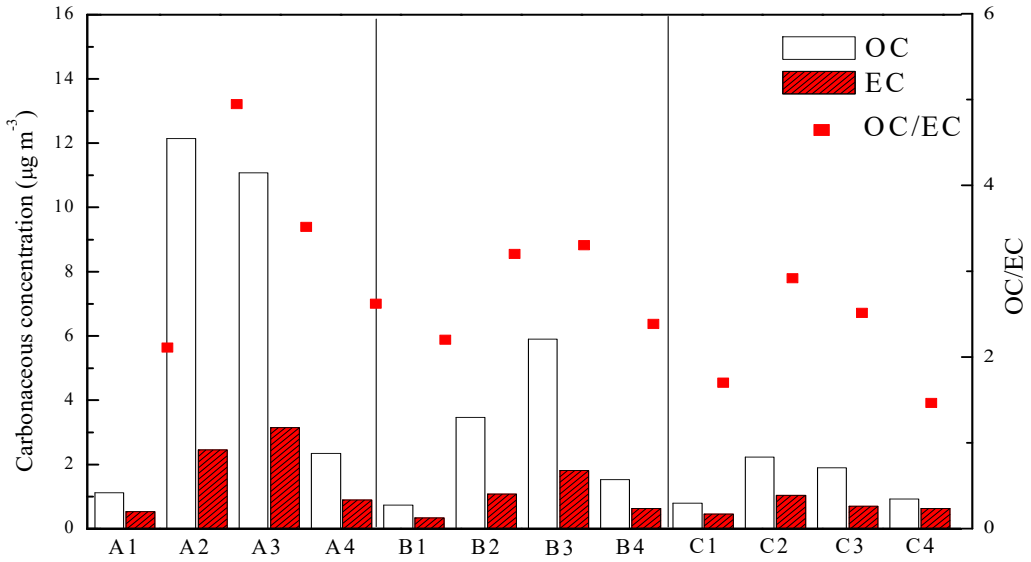

Fig. 5. Variation of daily carbonaceous concentrations at three sampling sites.

Analysis of Backward Trajectory

The analysis of backward trajectory is illustrated in Figs. S2(a)–2(d). It showed that on February 21st the air mass originating from Shandong Peninsula of mainland China successively passed through the Yellow Sea, the East China Sea, and the east coast of Taiwan Island before arriving at Taitung City. On February 22nd, the long-range transported air mass mainly came from the Yellow Sea and passed through the East China Sea before entering Taitung City, while a small amount of air mass originating from the north of Philippines, passed through the Bashi Channel and the Taiwan Strait, and landed at the north of Taiwan Island before entering Taitung City (see Fig. S2(b)). Since the air mass entering Hualien City, bounded on the north of Taitung City, originated from the same area and had the similar transport path as that entering Taitung City on February 22nd ((see Fig. S2(c)), the mean $PM_{2.5}$ concentration of Hualien City was 17.3 ± 4.2 μg m^{-3} for comparison, indicating that no episode occurred in Hualien City, and thus the air mass transported from the same area as that of Hualien City contributed little to the $PM_{2.5}$ pollution of Taitung City on February 22nd as well.

On February 23rd, the air mass originating from the Yellow Sea landed in the northern part of Taiwan through the East China Sea, and successively passed through Ilan, Hualien cities along the east side of the Central Range, and finally reached Taitung City (see Fig. S2(d)). Thus, the air mass might carry upwind $PM_{2.5}$ from the north to Taitung City. The daily mean $PM_{2.5}$ concentration of Hualien was 11.7 ± 3.7 μg m^{-3} on February 23rd, suggesting that no $PM_{2.5}$ episode occurred in the upwind of Taitung City. Therefore, the outside air mass had little influence on the $PM_{2.5}$ episode of Taitung City on February 23rd. On February 24th, the air masses mainly originated from the west coast of the Korean Peninsula, which had also little impact on the concentration of $PM_{2.5}$ in Taitung as well, since it passed through the Yellow Sea and the East China Sea before entering Taitung City (see Fig. S2(e)). Therefore, the $PM_{2.5}$ episode was mainly dominated by local sources in Taitung City instead of the air masses from outside region.

PMF Analysis

The PMF results of $PM_{2.5}$ source apportionment during the NDs showed that the emission sources of $PM_{2.5}$ included four main categories as shown in Fig. 6(a) and Table S1. In the Category I, Zn, EC, and OC had the highest loading, while Fe and Ca had moderately higher loading. Zinc is widely reported to be released by the wear of tires as mentioned, while EC and OC are primarily emitted by diesel and gasoline engine exhausts (Watson *et al.*, 2001; Cheng *et al.*, 2015; Corbin *et al.*, 2018; Li *et al.*, 2018). Metallic elements such as Fe, Ca, Mn, Cd, and Cu could be released

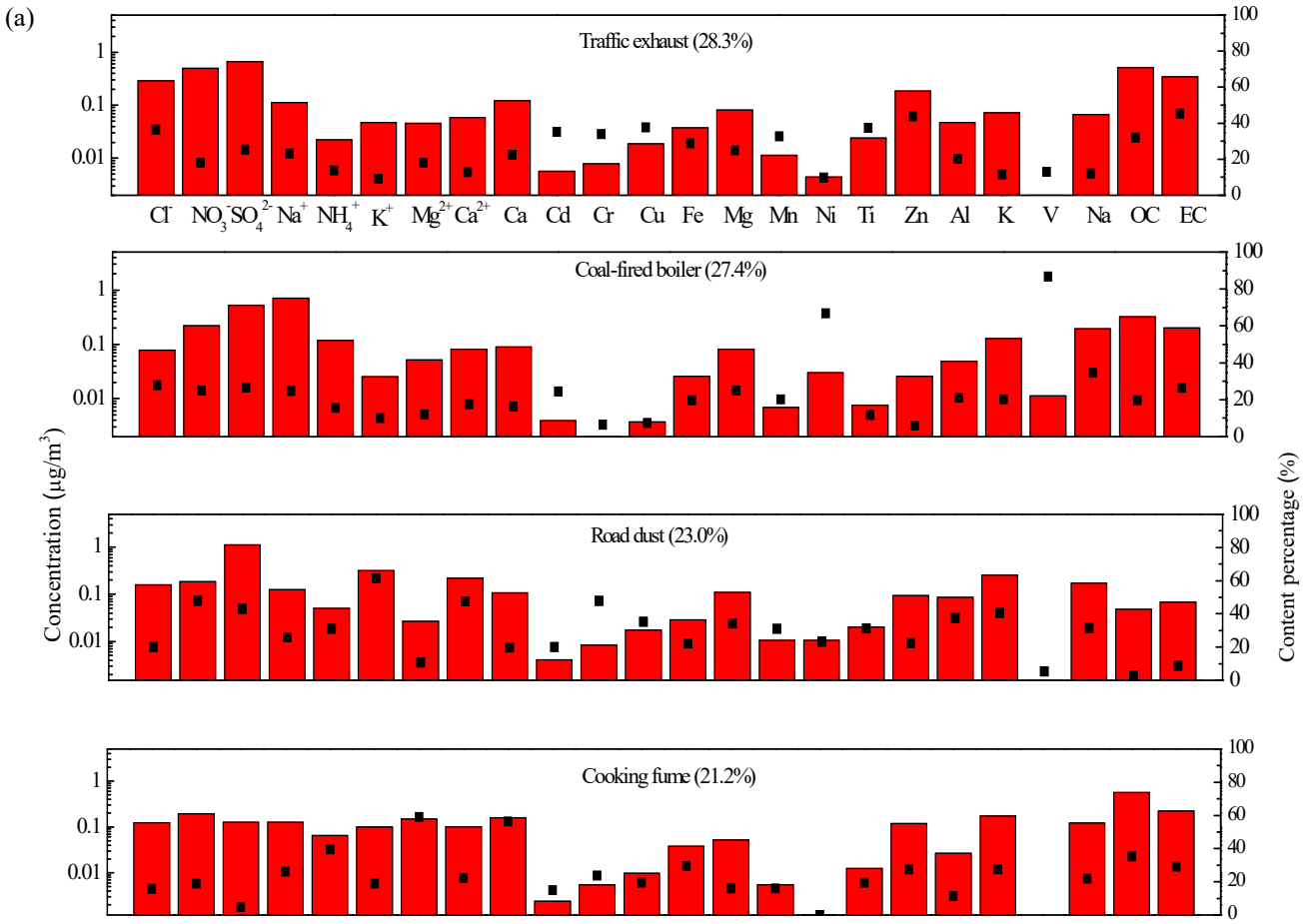

Fig. 6. Source profile and the loadings of chemical species during (a) the NDs and (b) the EDs by PFM analysis.

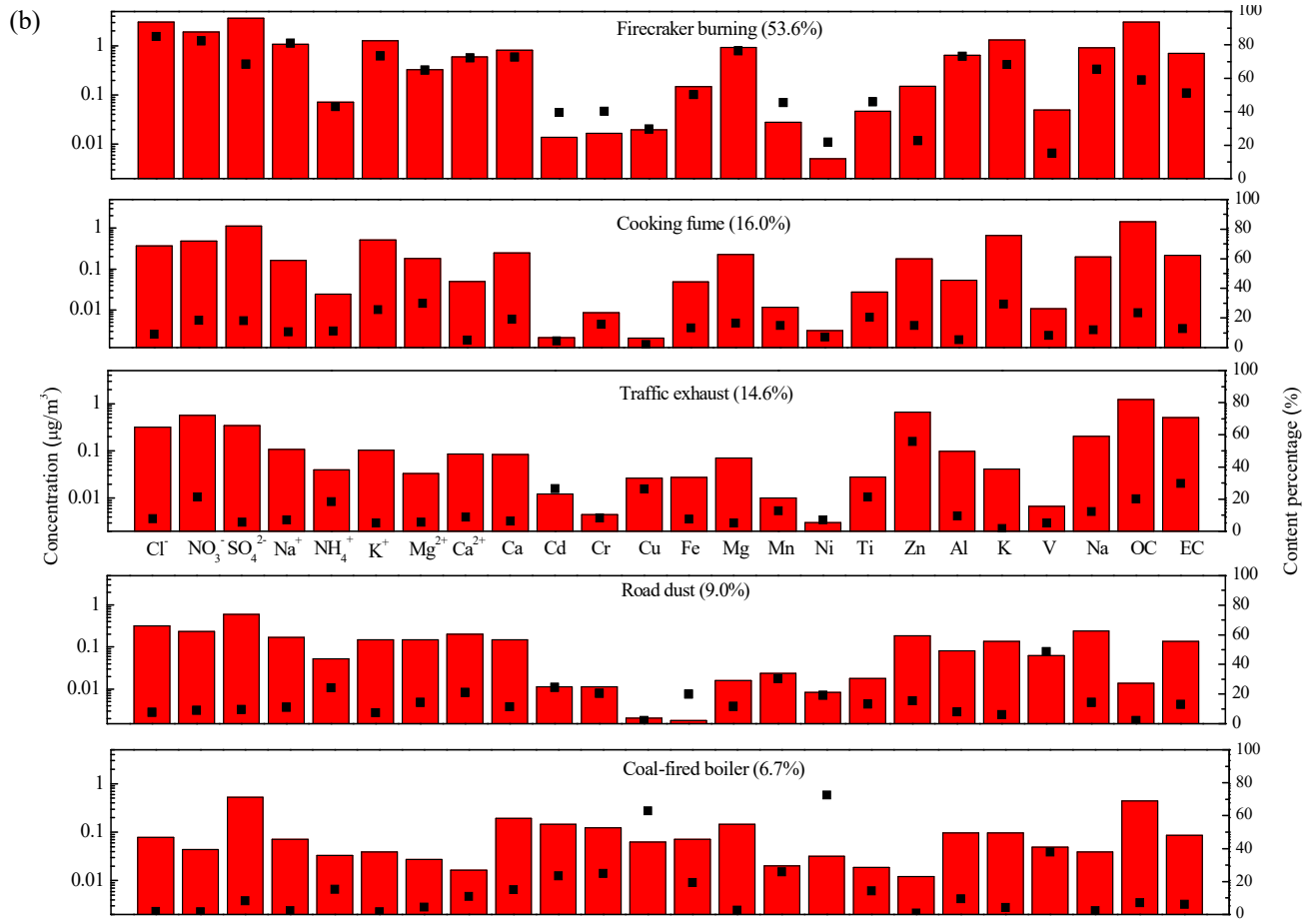

Fig. 6. (*continued*).

from the combustion of heavy oil (Li *et al.*, 2013b). Additionally, Fe and Ca could also be emitted by brake wear (Li *et al.*, 2013b). Thus, such a source profile was mainly attributed to the vehicular exhausts, and the determined mass of $PM_{2.5}$ was 3.2 μg m^{-3}, accounting for approximately 28.3% of the total mass of 11.3 μg m^{-3} analyzed by PMF. In Category II, the mean concentration of chemical species was 3.1 μg m^{-3}, accounting for 27.4% of the total mass. Ni, SO_4^{2-}, Mg^{2+}, Na^+, Cl^-, and NO_3^- were the dominant chemical species in Category II. In addition to Ni, which is mainly released by local coal-burning boilers as mentioned, V is also a metallic indicator of coal burning. SO_4^{2-} and Mg^{2+} are the essential chemical composition of coal-burning boilers as well (Sharp *et al.*, 2013; Pei *et al.*, 2016). Thus, the sources of these chemical species were attributed to coal-burning boilers. In Category III, the highest loading was identified as NO_3^-, SO_4^{2-}, Ca^{2+}, and K^+, and followed by NH_4^+, Mg, Ti, and Al, which were characterized as road dusts (Li *et al.*, 2012; Liu *et al.*, 2019). The mean concentration (2.6 μg m^{-3}) of $PM_{2.5}$ from the road dusts accounted for 23.0% of the total mass of $PM_{2.5}$. The chemical species with a total mass concentration of 2.4 μg m^{-3} in Category IV accounted for 21.2% of the total mass of $PM_{2.5}$. Mg^{2+}, Ca^{2+}, and OC had the highest loading among these species, while Na^+, Cl^-, K^+, and EC had higher loading. The composition highly matched the chemical feature of kitchen fumes (Li *et al.*, 2015).

A total of five source profile categories representing main $PM_{2.5}$ sources during the EDs is shown in Fig. 6(b). In the Category I, many chemical species including Cl^-, NO_3^-, SO_4^{2-}, Na^+, K^+, Mg^{2+}, Ca^{2+}, Ca, Fe, Mg, K, Na, OC, EC, Mn, Mg, and Al had high loadings, with a total mass of 20.1 μg m^{-3} accounting for 53.6% of the total average $PM_{2.5}$ concentration of 37.5 μg m^{-3} during the EDs, and thus, the chemical feature of the Category I could be attributed to the firecracker burning. What's more, the firecracker burning contributed approximately 76.7% of the increment of the average $PM_{2.5}$ concentrations (26.2 μg m^{-3}) between the NDs and the EDs. Therefore, firecracker burning played a vital role in the formation of $PM_{2.5}$ during the EDs. The pattern of the category II exhibited high loadings of OC, K^+, Mg^{2+}, and K, which were attributed to the feature of cooking fumes. Although the contribution percentage (16.0%) of the total mass of $PM_{2.5}$ was lower than that during the NDs, the concentration released from cooking fumes increased from 3.3 μg m^{-3} (NDs) to 6.0 μg m^{-3} (EDs) due to the dramatic increase of food stalls during the festival. In Category III, Zn, EC, and Ti had the highest loading among the chemical species, which was identified as the emission of vehicular exhausts, accounting for 14.6% of the total mass of $PM_{2.5}$. The mean concentration of 5.5 μg m^{-3} contributed by vehicles exhaust was slightly higher than that (4.5 μg m^{-3}) during the NDs due to the increase in the traffic flow of motor vehicles

Table 1. Health risks of heavy metals in $PM_{2.5}$ sampled at three sampling sites.

Elements	$Hl_{children}$			Hl_{adult}			Ri		
	A	B	C	A	B	C	A	B	C
Cd	9.37×10^{-6}	4.57×10^{-6}	4.38×10^{-6}	5.28×10^{-6}	2.58×10^{-6}	2.47×10^{-6}	1.67×10^{-7}	8.17×10^{-8}	7.83×10^{-8}
Cr	3.60×10^{-4}	3.17×10^{-4}	1.64×10^{-4}	2.03×10^{-4}	1.79×10^{-4}	9.38 × 10–5	1.21×10^{-6}	I.06 × 10^{-6}	5.58×10^{-7}
Cu	5.50×10^{-7}	4.50×10^{-7}	2.10×10^{-7}	3.10×10^{-7}	2.5×10^{-7}	1.20×10^{-7}	-	-	-
Fe	9.10×10^{-8}	1.10×10^{-7}	5.40×10^{-8}	5.10×10^{-8}	6.10×10^{-8}	3.10×10^{-8}	-	-	-
Mn	9.52×10^{-7}	1.01×10^{-6}	4.76×10^{-7}	5.37×10^{-7}	5.68×10^{-7}	2.68×10^{-7}	-	-	-
Ni	4.30×10^{-7}	0	2.00×10^{-7}	2.40×10^{-7}	0	1.10×10^{-7}	2.10×10^{-8}	0	9.80×10^{-9}
Zn	9.30×10^{-7}	4.90×10^{-7}	5.20×10^{-7}	5.22×10^{-7}	2.70×10^{-7}	2.90×10^{-7}	-	-	-
V	1.10 × 10–5	1.10×10^{-6}	4.40×10^{-7}	3.20×10^{-6}	6.21×10^{-7}	2.50×10^{-7}	-	-	-
HI_{Total} or R^t	3.70×10^{-4}	3.20×10^{-4}	1.84×10^{-4}	2.10×10^{-4}	1.83×10^{-4}	1.04×10^{-4}	1.39×10^{-6}	1.14×10^{-6}	6.46×10^{-7}

"-" means the results were unavailable due to the lack of SF_a.

along with the pilgrimage activities. NH_4^+, Ca^{2+}, and Mn showed the highest loading in Category IV, while Ni and V showed the highest loading in Category V, which originated from the fugitive road dust (8.1%) and local coal-fired boilers (6.1%), respectively. Correspondingly, their mean concentrations of 3.4 μg m^{-3} and 2.5 μg m^{-3} were lower than those during the NDs, indicating that the contributions of road dust and local coal-fired boilers to $PM_{2.5}$ decreased significantly during the EDs. To sum up, a small portion (13.6%) of the increment was contributed by cooking fume and vehicles exhaust, while the contribution to the increment was nearly zero by local coal-fired boilers.

Risk Assessment

The hazard quotients (HQs) of heavy metals in $PM_{2.5}$ for children and adults at sites A, B, and C on February 22nd were compared and summarized in Table 1. The HI_{total} of heavy metals for children and adults at each site was lower than the accepted risk threshold of unity, indicating that the heavy metals in $PM_{2.5}$ were unlikely to cause noncarcinogenic risk on the spectators in the vicinity of firecracker burning site during the EDs. The HI_{total} of heavy metals at site A for children (3.70×10^{-4}) and adults (2.10×10^{-4}) was higher than those of 3.20×10^{-4} and 1.83×10^{-4} at site B, respectively. While the HI_{total} for children (1.84×10^{-4}) and adults (1.04×10^{-4}) at site C were the lowest at the three sites since site C was far away from the firecracker burning site. These results indicate that the HI_{total} of heavy metals varied significantly with the downwind distance to the firecracker burning site. Additionally, the HI_{total} of heavy metals for children was generally higher than that for adults, indicating that children were more susceptible to the health hazards of firecracker burning. It was noted that the highest risk level for these heavy metals was attributed to Cr ranging from 0.93×10^{-4} to 3.60×10^{-4}, which was mainly released by the occasional burning of small fireworks, namely, the HI_{total} of heavy metals was not directly associated with the firecracker burning. However, a large amount of SO_2, NO_x, CO, and other organic matter released from the firecracker burning are harmful to humans' health, which needs further investigation (Greven *et al.*, 2019).

The comparison of the carcinogenic risk values (R_t) of heavy metals at each site showed that, during the EDs, the R_t values at sites A and B were 1.21×10^{-6} and 1.06×10^{-6}, respectively, which were higher than the carcinogenic risk threshold of 1.00×10^{-6}. Therefore, a possible carcinogenic risk to the spectators on sites A and B can not be neglected due to the firecracker burning. The R_t value at site C was 0.58×10^{-6}, which was lower than the threshold, indicating that the carcinogenic risk to the residents in the vicinity of site C was lower than those at sites A and B due to its long downwind distance to the firecracker burning site. Besides, the largest R_i was contributed by Cr (0.58×10^{-6}–1.21×10^{-6}) as well. It is noted that the cancer risk of PAHs in $PM_{2.5}$ should not be neglected (Fan *et al.*, 2017). Nevertheless, the cancer risk of heavy metals in $PM_{2.5}$ estimated via the chronic daily intake is usually far higher than those of PAHs (Christopher *et al.*, 2018). Thus, this study did not investigate the health risk of PAHs.

CONCLUSIONS

During the EDs, the downwind distance to the burning site presented a significant impact on the spatial distribution of the chemical composition of $PM_{2.5}$. The increments of both the contents and concentrations of metallic elements, WSI, carbonaceous species at site A were significantly higher than those at sites B and C, which were located far away from the firecracker burning site. The main sources of $PM_{2.5}$ during the EDs were the firecracker burning, kitchen fumes, and vehicles exhaust, while the increment contributed by local coal-fired boilers was far lower than those during the NDs. During the EDs, the metallic elements in $PM_{2.5}$ had low noncarcinogenic risk to residents living in the vicinities of the sampling sites. However, the carcinogenic risk was highly influenced by the downwind distance to the burning site. The carcinogenic risk at the site close to the firecracker burning site was higher than the carcinogenic risk threshold, while that far away from the burning site was lower than the carcinogenic risk threshold.

ACKNOWLEDGEMENTS

This study was performed under the auspices of the Ministry of Science and Technology, Taiwan, under the contract number of NSC105-EPA-F-009-002 and National Natural Science Foundation of China, under the contract number of 21477042. The authors are grateful to their

financial supports in order to accomplish this study.

SUPPLEMENTARY MATERIAL

Supplementary data associated with this article can be found in the online version at http://www.aaqr.org.

REFERENCES

Alexandre, J., Audrey, S., Tom, K., Michel, F., Ewa, D., Valbona, C., Daivd, M., Rene, S., Real, D., Alain, M. and Jeffrey, B. (2015). Spectroscopic investigation of $PM_{2.5}$ collected at industrial, residential and traffic sites in Taif, Saudi Arabia. *J. Aerosol Sci.* 79: 97–108.

Chen, Y., Schleicher, N., Cen, K., Liu, X., Yu, Y., Zibat, V., Dietze, V., Fricker, M., Kaminski, U., Chen, Y., Chai, F. and Norra, S. (2016). Evaluation of impact factors on $PM_{2.5}$ based on long-term chemical components analyses in the megacity Beijing, China. *Chemosphere* 155: 234–242.

Cheng, Y., Lee, S.C. and Gu, Z.L. (2015). $PM_{2.5}$ and $PM_{10\text{-}2.5}$ chemical composition and source apportionment near a Hong Kong roadway. *Particulogy* 18: 96–104.

Choosong, T., Chomanee, J., Tekasakul, P., Tekasakul, S., Otani, Y., Hata, M., Furuuchi, M. (2010). Workplace environment and personal exposure of PM and PAHs to workers in natural rubber sheet factories contaminated by wood burning smoke. *Aerosol Air Qual. Res.* 10: 8–21.

Christopher, L., Farimah, S., Mohammad, H.S. and Constantinos, S. (2018) Commuting in Los Angeles: Cancer and non-cancer health risks of roadway, light-rail and subway transit routes. *Aerosol Air Qual. Res*. 18: 2363–2374.

Corbin, J.C., Mensah, A.A. and Michalke, B. (2018). Trace metals in soot and $PM_{2.5}$ from heavy-fuel-oil combustion in a marine engine. *Environ. Sci. Technol.* 52: 6714–6722.

Fan, Z.L., Chen, X.H., Lui, K.H., Ho, H.S., Cao, J.J., Lee, S.C., Huang, H. and Ho, K.F. (2017). Relationships between outdoor and personal exposure of carbonaceous species and polycyclic aromatic hydrocarbons (PAHs) in fine particulate matter ($PM_{2.5}$) at Hong Kong. *Aerosol Air Qual. Res*. 17: 666–679.

Fang, G.C. and Chang S.C. (2010). Atmospheric particulate (PM_{10} and $PM_{2.5}$) mass concentration and seasonal, variation study in the Taiwan area during 2000-2008s. *Atmos. Res.* 98: 368–377.

Feng, J.L., Sun, P., Hu, X.L., Zhao, W., Wu, M.H. and Fu, J.M. (2012). The chemical composition and sources of $PM_{2.5}$ during the 2009 Chinese New Year's holiday in Shanghai. *Atmos. Res.* 118: 435–444.

Feng, J.L., Hao, Y., Su, X.F., Liu, S.H., Li, Y., Pan, Y.P. and Sun, J.H. (2016). Chemical composition and source apportionment of $PM_{2.5}$ during Chinese Spring Festival at Xinxiang, a heavily polluted city in North China: Fireworks and health risks. *Atmos. Res.* 182: 176–188.

Greven, F.E., Judith, M., Fischer, V.P., Duijm, F., Vink, N.M. and Brunekreef, B. (2019). Air pollution during New Year's fireworks and daily mortality in the Netherlands. *Sci. Rep.* 9: 5735.

Han, Z., Jiang, Q., Du, Z., Huey, H.H., Yu, Y., Zhang, Y., Li, G. and Sun, Y. (2019). A novel environmental-friendly and safe unpacking powder without magnesium, aluminum and Sulphur for fireworks. *J. Hazard. Mater.* 373: 835–843.

Hjortenkrans, D.S., Bergbäck, B.G. and Häggerud, A.V. (2007). Metal emissions from brake linings and tires: case studies of Stockholm, Sweden, 1995/1998 and 2005. *Environ. Sci. Technol.* 41: 5224–5230.

Jiang, Q., Sun, Y.L., Wang, Z. and Yin, Y. (2015). Aerosol composition and sources during the Chinese Spring Festival: Fireworks, secondary aerosol, and holiday effects. *Atmos. Chem. Phys.* 15: 6023–6034.

Jung, J., Lee, D., Jeong, H, Lee, S. and Oh, S.H. (2018). Chemical characterization of the long-range transport of firework/firecracker emissions over the Korean Peninsula: A novel indicator of Asian continental outflows. *Atmos. Environ.* 178: 223–230.

Kong, S.F., Li, L., Li, X.X., Yin, Y., Chen, K., Liu, D.T., Yuan, L., Zhang, Y.J., Shan, Y.P. and Ji, Y.Q. (2015). The impacts of firework burning at the Chinese Spring Festival on air quality: Insights of tracers, source evolution and aging processes. *Atmos. Chem. Phys.* 15: 2167–2184.

Lee, Y.Y., Wang, L.C., Zhu, J.N., Wu, J.L. and Lee, K.L. (2018). Atmospheric $PM_{2.5}$ and polychlorinated dibenzo-*p*-dioxins and dibenzofurans in Taiwan. *Aerosol Air Qual. Res.* 18: 762–779.

Li, M.R., Hu, M., Guo, Q.F., Tian, T.Y., Du, B.H., Huang, X.F., He, L.Y., Guo, S., Wang, W.F., Fan, Y.G. and Xu, D.D. (2018). Seasonal source apportionment of $PM_{2.5}$ in Ningbo, a coastal city in southeast China. *Aerosol Air Qual. Res.* 18: 2741–2752.

Li, T.C., Chen, W.H., Yuan, C.S., Wu, S.P. and Wang, X.H. (2013a). Physicochemical characteristics and source apportionment of atmospheric particles in Kinmen-Xiamen Airshed. *Aerosol Air Qual. Res.* 13: 308–323.

Li, T.C., Yuan, C.S., Huang, H.C., Lee, C.L., Wu, S.P. and Tong, C. (2017a). Clustered long-range transport routes and potential sources of $PM_{2.5}$ and their chemical characteristics around the Taiwan Strait. *Atmos. Environ.* 148: 152–166.

Li, Y.C., Yu, J.Z., Ho, S.S.H., Yuan, Z., Lau, A.K.H. and Huang, X.F. (2012). Chemical characteristics of $PM_{2.5}$ and organic aerosol source analysis during cold front episodes in Hong Kong, China. *Atmos. Res.* 118: 41–51.

Li, Y.C., Yu, J.Z., Ho, S.S.H., Yuan, Z., Schauer, J.J., Lau, A.K.H. and Louie, P.K.K. (2013b). Chemical characteristics and source apportionment of fine particulate organic carbon in Hong Kong during high particulate matter episodes in winter 2003. *Atmos. Res.* 120: 88–98.

Li, Y.C., Man, S., Steven, S., Wang, C., Cao, J.J., Wang, G.H., Wang, X.X., Wang, K. and Zhao, X.Q. (2015). Characteristics of $PM_{2.5}$ emitted from different cooking activities in China. *Atmos. Res.* 166: 83–92.

Li, Y.Y., Yang, L.X., Chen, X.F., Gao, Y., Jiang, P., Zhang, J.M., Yu, H. and Wang, W.X. (2017b). $PM_{2.5}$-bound PAHs in indoor and outdoor of hotels in urban and suburban of Jinan, China: Concentrations, sources, and health risk impacts. *Aerosol Air Qual. Res*. 17: 2463–

2473.

Lin, C.C. (2016). A review of the impact of fireworks on particulate matter in ambient air. *J. Air Waste Manage. Assoc.* 66: 1171–1182.

Lin, N.H., Tsay, S.C., Maring, H.B., Yen, M.C., Sheu, G.R., Wang, S.H., Chi, K.H., Chuang, M.T., Yang, C.F., Fu, J.S., Reid, J.S., Lee, C.T., Wang, L.C., Wang, J.L., Hsu, C.N., Sayer, A.M., Holben, B.N., Chu, Y.C. and Anh, X. (2013). An overview of regional experiments on biomass burning aerosols and related pollutants in Southeast Asia: From BASE-ASIA and the Dongsha Experiment to 7-SEAS. *Atmos. Environ.* 78: 1–19.

Liu, J.W., Chen, Y.J., Chao, S.H., Cao, H.B. and Zhang, A.C. (2019). Levels and health risks of $PM_{2.5}$-bound toxic metals from firework/firecracker burning during festival periods in response to management strategies. *Ecotoxicol. Environ. Saf.* 171: 406–413.

Lough, G.C., Schauer, J.J. and Park, J.S. (2005). Emissions of metals associated with motor vehicle roadways. *Environ. Sci. Technol.* 39: 826–836.

Moreno, T., Querol, X., Alastuey, A., Cruz Minguillon, Pey, M., Vicente, Miro, Filis, C. and Gibbons, W. (2007). Recreational atmospheric pollution episodes: Inhalable metalliferous particles from firework displays. *Atmos. Environ.* 41: 913–922.

Mukherjee, T., Asutosh, A., Pandey, K.S., Yang, L., Gogoi, P.P., Panwar, A. and Vinoj V. (2018). Increasing potential for air pollution over megacity New Delhi: A study based on 2016 Diwali episode. *Aerosol Air Qual. Res*. 18: 2510–2518.

Pei, B., Wang, X.L. and Zhang, Y.H. (2016). Emissions and source profiles of $PM_{2.5}$ for coal-fired boilers in the Shanghai megacity, China. *Atmos. Pollut. Res.* 7: 577–584.

Rastogi, N., Singh, A. and Satish, R. (2019). Characteristics of submicron particles coming from a big firecracker burning event: Implications to atmospheric pollution. *Atmos. Pollut. Res.* 10: 629–634.

Ravindra, K., Mor, S. and Kaushik, C.P. (2003). Short-term variation in air quality associated with firework events, a case study. *J. Environ. Monit.* 5: 260-264.

Sharp, A. and Turner, A. (2013). Concentrations and bioaccessibilities of trace elements in barbecue charcoals. *J. Hazard. Mater.* 262: 620–626.

Song, Y., Zhang, Y., Xie, S., Zeng, L., Zheng, M., Salmom, L.G., Shao, M. and Slanina, S. (2006). Source apportionment of $PM_{2.5}$ in Beijing by positive matrix factorization. *Atmos. Environ.* 40: 1526–1537.

Song, Y., Wan, X.M., Bai, S.X., Guo, D., Ren, C., Zeng, Y., Li, Y.R. and Li, X.W. (2017). The characteristics of air pollutants during two distinct episodes of fireworks burning in a valley city of North China. *PLoS One* 12: e0168297.

Tian, Y.Z., Wang, J., Peng, X., Shi, G.L. and Feng, Y.C. (2014). Estimation of the direct and indirect impacts of fireworks on the physicochemical characteristics of atmospheric PM_{10} and $PM_{2.5}$. *Atmos. Chem. Phys.* 14: 9469–9479.

Tsai, H.H., Yuan, C.S., Hung, C.H. and Lin, Y.C. (2010). Comparing physicochemical properties of ambient particulate matter of hot spots in a highly polluted air quality zone. *Aerosol Air Qual. Res.* 10: 331–344.

Tsai, H.H., Chien, L.H., Yuan, C.S., Lin, Y.C., Jen, Y.H. and Ie, I.R. (2012). Influences of fireworks on chemical characteristics of atmospheric fine and coarse particles during Taiwan's lantern festival. *Atmos. Environ.* 62: 256–264.

U.S. EPA (2014). EPA positive matrix factorization (PMF) 5.0 Fundamentals and User Guide, 2014.

Vecchi, R., Bernardoni, V., Cricchio, D., D'Alessandro, A., Fermo, P. and Lucarelli, F. (2008). The impact of fireworks on airborne particles. *Atmos. Environ.* 42: 1121–1132.

Wang, Q.Y., Cao, J.J., Shen, Z.X., Tao, J., Xiao, S., Luo, L., He, Q.Y. and Tang, X.Y. (2013). Chemical characteristics of $PM_{2.5}$ during dust storms and air pollution events in Chengdu, China. *Particuology* 11: 70–77.

Wang, Y., Zhuang, G., Xu, C. and An, Z. (2007). The air pollution caused by the burning of fireworks during the lantern festival in Beijing. *Atmos. Environ*. 41: 417–431.

Watson, J.G., Chow, J.C. and Houck, J.E. (2001). $PM_{2.5}$ chemical source profiles for vehicle exhaust, vegetative burning, geological material, and coal burning in Northwestern Colorado during 1995. *Chemosphere* 43: 1141–1151.

Wu, S.P., Schwab, J., Yang, B.Y., Zheng, A. and Yuan, C.S. (2015). Two-year $PM_{2.5}$ observations at four urban sites along the coastlines of Southeastern China. *Aerosol Air Qual. Res*. 15: 1799–1812.

Yang, H., Chen, J., Wen, J., Tian, H. and Liu, X. (2015). Composition and sources of $PM_{2.5}$ around the heating periods of 2013 and 2014 in Beijing: implications for efficient mitigation measures. *Atmos. Environ.* 124: 378–386.

Yang, H.Y., Tseng, Y.L., Chuang, H.L., Li, T.C., Yuan, C.S. and Lee, J.J. (2017). Chemical fingerprint and source identification of atmospheric fine particles sampled at three environments at the tip of southern Taiwan. *Aerosol Air Qual. Res.* 17: 529–542.

Yang, L.X., Gao, X.M., Wang, X.F., Nie, W., Wang, J., Gao, R., Xu, P.J., Shou, Y.P., Zhang, Q.Z. and Wang W.X. (2014). Impacts of firecracker burning on aerosol chemical characteristics and human health risk levels during the Chinese New Year Celebration in Jinan. China. *Sci. Total Environ.* 476–477: 57–64.

Yang, S., Ma, Y.L., Duan, F.K., He, K.B., Wang, L.T., Wei, Z., Zhu, L.D., Ma, T., Li H. and Ye, S.Q. (2018). Characteristics and formation of typical winter haze in Handan, one of the most polluted cities in China. *Sci. Total Environ.* 613–614: 1367–1375.

Yuan, C.S., Lee, C.G., Liu, S.H., Chang, J.C., Yuan, C. and Yang, H.Y. (2006). Correlation of atmospheric visibility with chemical composition of Kaohsiung aerosols. *Atmos. Res.* 82: 663–679.

Zhang, J., Yang, L., Chen, J., Mellouki, A., Jiang, P., Gao, Y., Li, Y., Yang, Y. and Wang, W. (2017a). Influence of fireworks displays on the chemical characteristics of $PM_{2.5}$ in rural and suburban areas in Central and East China. *Sci. Total Environ.* 578: 476–484.

Zhang, J., Lance, S., Freedman, J.M., Sun, Y.L., Crandall, B.A., Wei, X.L. and Schwab, J.J. (2018a). Fine particles from Independence Day fireworks events: Chemical characterization and source apportionment. *Atmos. Chem. Phys. Discuss.* https://doi.org/10.5194/acp-2018-529

Zhang, J., Wu, L., Fang, X.Z., Li, F.H., Yang, Z.W., Wang, T., Mao, H.J. and Wei, E.Q. (2018b). Elemental composition and health risk assessment of PM_{10} and $PM_{2.5}$ in the roadside microenvironment in Tianjin, China. *Aerosol Air Qual. Res.* 18: 1817–1827.

Zhang, Y.Y., Wei, J.M., Tang, A.H., Zheng, A.H., Shao, Z.X. and Liu, X.J. (2017b). Chemical Characteristics of $PM_{2.5}$ during 2015 Spring Festival in Beijing, China. *Aerosol Air Qual. Res.* 17: 1169–1180.

Received for review, August 24, 2019
Revised, September 24, 2019
Accepted, September 24, 2019